Sensors and Actuators B 210 (2015) 75–81

Contents lists available at ScienceDirect

Sensors and Actuators B: Chemical

journal homepage: www.elsevier.com/locate/snb

Nanosheets assembled hierarchical flower-like WO_3 nanostructures: Synthesis, characterization, and their gas sensing properties

Chong Wang, Xin Li, Changhao Feng, Yanfeng Sun*, Geyu Lu*

State Key Laboratory on Integrated Optoelectronics, College of Electronic Science and Engineering, Jilin University, 2699 Qianjin Street, Changchun 130012, PR China

ARTICLE INFO

Article history:
Received 14 October 2014
Received in revised form 3 December 2014
Accepted 7 December 2014
Available online 13 December 2014

Keywords:
WO_3
Hierarchical nanostructure
Flower-like
NO_2 sensor

ABSTRACT

A three-dimensional hierarchical WO_3 nanostructure with a novel nanosheet-assembled morphology was synthesized through acidification of $Na_2WO_4{\cdot}2H_2O$. Firstly, precipitate got from $Na_2WO_4{\cdot}2H_2O$ and HCl was used as precursor. Secondly, the precursor was pretreated by concentrated acid for 24 h. Thirdly, deionized water was poured into the above solution directly to form the final products. The results revealed that the pretreatment by using high-concentration acid is the crucial factor in order to obtain the flower-like nanostructures. The WO_3 samples were characterized by X-ray diffraction analysis (XRD), scanning electron microscopy (SEM), transmission electron microscopy (TEM) and Brunauer–Emmett–Teller (BET). The results revealed that the samples were flower-like structure. The subunits of the flower-like nanostructures are ultrathin nanosheets with a thickness of about 20 nm. Sensors based on the synthesized WO_3 exhibited high response to NO_2. The detection limit can be as low as ~40 ppb level. Such novel WO_3 nanostructures may be a promising material for sensor application in detecting NO_2.

1. Introduction

With the rapid development of industry, the hazardous gases have become a serious problem which is harmful to human health and safety [1]. NO_2, as one kind of toxic gases, can cause photochemical smog and acid rain [2]. In addition, it could affect human health even at part per million (ppm) levels, such as respiratory system and nerve system [3]. The Occupational Safety and Health Administration (OSHA) have set a permissible exposure levels for NOx by 5 ppm [4], and the threshold concentration of NO_2 in air is 3 ppm as listed in the safety standards by the American Conference of Governmental Industrial Hygienists [5]. Thus, there is a strong demand for developing cheap, reliable and sensitive gas sensors targeting NO_2. Based on this criterion, chemical gas sensor with high performance has functioned in environmental monitoring and industrial production safety. Recently, metal oxide nano/microstructure gas sensors have attracted much attention owing to their high sensitivity, low cost and high response [6–8]. As a result, many kinds of metal oxide nano/microstructures have been developed, such as ZnO [9], SnO_2 [10] and CuO [11].

WO_3 is an important semiconducting material with good sensing properties toward NO_2 gas among these gas sensing materials studied so far [12]. With the going deep of the research work, WO_3 with different dimensional nanostructures have been synthesized in order to improve the performance of devices, such as nanowire [13], nanoplate [14], hollow-sphere [15], urchin-like [16] and many other hierarchically complex micro/nanostructures [17–20]. Specially, hierarchical nanostructures using lower dimension nanocrystals as the building blocks attract more interest due to their less gas diffusion length, higher mobility, and relatively larger specific surface area than the agglomerated nanoparticles [21]. Therefore, developing new and high-efficient 3D hierarchical microstructures for the gas-sensing applications is an imperative and challenging mission. Up to now, a variety of routes have been employed to obtain WO_3 crystal such as chemical vapor deposition [22], electrodeposition [23], template method [24] and hydrothermal method [25]. Despite the different methods discussed, it still remains a challenge for researchers to develop a facile and low-temperature wet chemical route to synthesize shape-selective WO_3 hierarchical nanostructures that does not use any toxic reagents or any organic additives.

In this work, nanosheets assembled hierarchical flower-like WO_3 were successfully synthesized through an acid treated method at 40 °C without using any organic additives. Moreover, the pretreatment to the precursor by concentrated acid was found to be

---

* Corresponding authors. Fax: +86 431 85167808.
E-mail addresses: syf@jlu.edu.cn (Y. Sun), lugy@jlu.edu.cn (G. Lu).

http://dx.doi.org/10.1016/j.snb.2014.12.020
0925-4005/

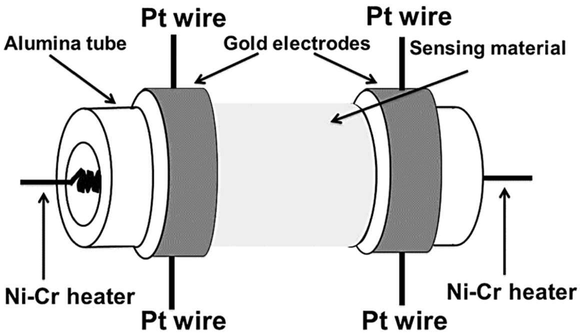

Fig. 1. Schematic structure of the gas sensor.

crucial to control the morphology of the final products. This kind of processing method and thus obtained novel nanostructured WO_3 has been reported in the literature rarely to our best knowledge. The flower-like nanostructures-based gas sensor showed high sensing performances. These results are promising for further application of hierarchical nanostructures as gas sensor.

2. Experimental

All the reagents (analytical-grade purity) were used without any further purification.

1 g $Na_2WO_4{\cdot}2H_2O$ was dissolved in 20 ml deionized water to form transparent solution with mild stirring. Then, 2 M HCl was added into the solution drop by drop. The pale yellow precipitate was formed when enough HCl was added. The gel was washed with deionized water and ethanol by centrifugation for several times. After that, the precursor was pretreated by 60 ml of 12 M HCl solution at 40 °C with stirring. 24 h later, the solution became clear. Then, 30 ml deionized water was added into the above solution to keep stirring for another 9 h. The obtained precipitates were washed with deionized water and ethanol by centrifugation for several times and dried at 80 °C for 10 h. Finally, the precipitates were sintered at 500 °C to get the WO_3 sample.

A sensor device was fabricated using the obtained WO_3 powder. Firstly, a suitable amount of WO_3 powder was mixed with ethanol to obtain a paste which was then coated onto an alumina tube (4 mm in length, 1.2 mm in external diameter and 0.8 mm in internal diameter) using a small brush slowly and lightly. The tube was installed with a pair of gold electrodes, and each electrode was connected with two Pt wires. After drying in air for a while, the thin film with proper thickness was formed. Then the tube was placed in a muffle furnace and the temperature was kept at 300 °C for 2 h. When the temperature was reduced to room temperature, the tube with sensing film was soldered to the pedestal. Finally, a Ni–Cr alloy coil was inserted into the alumina tube as a heater in order to control the operating temperature of the sensor. The structure of the sensor is shown in Fig. 1 Fig. 1. The electrical resistance of the sensor was measured in air and in target gas, respectively. The response of the sensor is defined as $S = Rg/Ra$ for oxidizing gas or Ra/Rg for reducing gas, here, Ra and Rg are the resistances of the sensor in the air and target gas, respectively. The response time and recovery time are defined as the time taken by the sensor to achieve 90% of the total resistance change during the adsorption and desorption process, respectively.

The crystal phase and morphologies of the acid-treated products and calcined products were observed by X-ray powder diffraction (XRD, Rigaku D/max-2550) with Cu Kα1 radiation ($\lambda = 0.15406$ nm) at 50 kV/200 mA and the scanning speed was 12°/min, field emission scanning electron microscopy (SEM, JEOL JSM-7500F, 15 kV), high resolution transmission electron microscopy (HRTEM, JEM 2100F, 200 kV), Brunauer–Emmett–Teller (BET), and selected area electron diffraction (SAED). Thermogravimetric (TG) analysis and differential scanning calorimetric (DSC) measurements were also carried out using a NETZSCH STA 449F3 simultaneous thermogravimetric analyzer under air atmosphere in the temperature range from 30 to 800 °C with a heating rate of 10 °C min^{-1}.

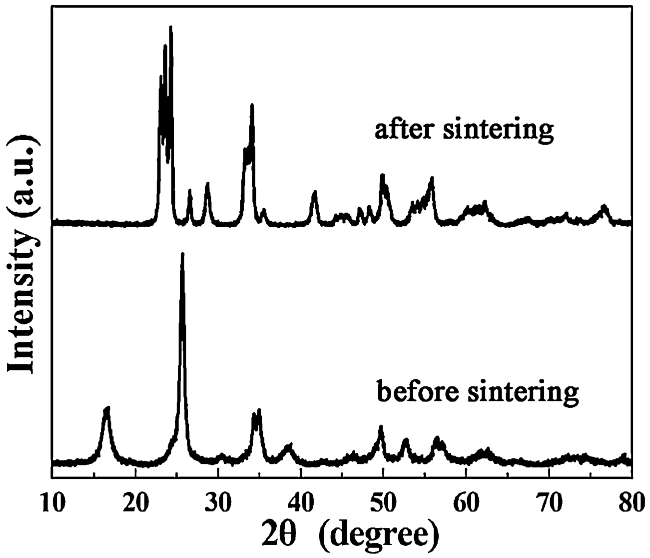

Fig. 2. X-ray diffraction patterns of the as-prepared samples before and after sintering.

3. Results and discussion

3.1. Structural and morphological characteristics of the prepared WO_3

The XRD patterns of samples before and after sintering are given in Fig. 2. It can be seen that before sintering (Fig. 2b), all the diffraction peaks could be indexed to $H_2W_4O_{13}$ (JCPDS file no. 1-583). No peaks of other impurity phases are detected from this pattern. And after sintering at 500 °C, $H_2W_4O_{13}$ was converted into pure monoclinic structure of WO_3 according to JCPDS card no. 89-4476. No characteristic peaks from any other impurities can be observed, indicating that no impurity exists and the $H_2W_4O_{13}$ have completely transformed into the monoclinic WO_3 phase after sintering.

The morphologies and microstructures of the samples before and after sintering are illustrated by FESEM observations. Fig. 3a shows the morphology of the sample before sintering, from which abundant nanosheets-assembled flower-like nanostructures with good monodispersity and uniformity are observed clearly. No other morphologies can be detected from the panoramic FESEM image, indicating a high yield of these nanostructures. The enlarged FESEM image shown in Fig. 3b reveals that the entire structure of the 3D hierarchical architecture is constructed with dozens of 2D nanosheets with a smooth surface. These nanosheets with regular edge connect to each other through the center to form 3D hierarchical structure. As shown in Fig. 3c, the WO_3 sample retains the morphology and size of $H_2W_4O_{13}$ precursor after sintering at 500 °C. The detail morphology information can be found in Fig. 3d. It can be observed that the thickness of the ultrathin nanosheets is about 20 nm. In addition, the edge of the nanosheets became a little irregular compared to the $H_2W_4O_{13}$ precursor. The image of products obtained without the pretreatment by concentrated acid is shown in Fig. 3e. Only some irregular-shaped nanosheets can be observed. This difference proves the importance of the pretreatment by concentrated acid, which is crucial to control the morphology of the final products.